Impact of Water Seepage of New Suez Canal on Soil Properties of El-Amal Area, Ismailia East, Egypt

Adel A. Elwan

Pedology Department, Water Resources and Desert Soils Division, Desert Research Center, Cairo, 11753, Egypt

Received: *5/3/2021*

Abstract: Seawater seepage poses a major problem for agriculture in Egypt's coastal areas. In 2020, a 285 Faddan area in El-Amal, Ismailia East was selected as a representative soil model for Egypt's New Suez Canal region to investigate the impact of seawater seepage on soil properties and identify the responsible factors for land degradation, with an emphasis on suitable adaptations to land limitations and climate stressors. Seawater changes the behavior of soil and creates geotechnical problems that enhance soil alkalinity and salinity value. Five soil mapping units (SMUs) were identified with moderately to shallow soils dominating, in a detailed soil survey that was conducted in the field to conduct pedomorphological and physicochemical investigations. The water table had raised by 50–100 cm within the soil pedons. Approximately 45.4 Faddans were recognized as sabkhas due to the inundation of lowlands with seawater. Most study lands (217.2 Faddan) were unsuitable for cultivation due to the higher limitations of salinity, alkalinity, soil structure, and poor drainage under saturation conditions. The salinity of saturated soil reached 29.60 dS/m, posing a major challenge to agriculture. The results indicated that the pedomorphological and physicochemical properties of most study soils had degraded and become unsuitable for cultivation, which was linked to the seawater seepage. It is predicted that the rest lands (SMU1 and SMU2) and other adjacent lands to the study area are expected to change into desertified lands in the future due to continuous seawater seepage. The New Suez Canal's seawater seepage caused the cultivated fruit trees and other vegetation in the study area to dry up and die. Climate change-induced seawater seepage and drought were the direct causes of soil salinization in the study lands. To achieve long-term sustainability and avoid maladaptive outcomes, an urgent need to adopt an integrated approach for large-scale investments in Egypt's farming sector is urgently needed for effective policymaking toward achieving food security, with it being recognized that climate change has adverse effects and challenges to the soil resources in Egypt, and therefore, the sustainable planning of natural resources in coastal areas should be further studied and thoroughly managed. Adopting local adaptation actions and strategies for incremental, systemic, and transformational changes at the farm and on large scales in the agricultural sector is critical. The transformational adaptation actions are the suitable practices, followed by incremental and systemic adaptations to combat the agricultural limitations and climate change stressors in the current study lands.

Keywords: Seawater seepage, Climate change adaptation, Soil degradation, New Suez Canal, Egypt

INTRODUCTION

Nowadays, climate change increases major challenges regarding the sustainable utilization of natural resources in coastal arid areas (Omar *et al.,* 2021). The natural resources of soil and water in Egypt are extremely vulnerable to major challenges of climate change and their agricultural sustainability. Egypt could run out of freshwater resources by the year 2025 as recently reported by the United Nations (WMO, 2017; Yassen *et al.,* 2020). Global climate change can affect the surface temperature of the atmosphere and rainfall patterns causing drought or flash flooding worldwide (Shalby *et al.,* 2021). This can cause disturbances in groundwater hydraulics and increase seawater seepage in the coastal agricultural land and groundwater aquifers particularly in Egypt (Ketabchi *et al.,* 2016; Omar *et al.,* 2021). Globally, the air temperature is augmented (Zhang *et al.,* 2021) and the global atmosphere become warmer by 0.5°C during the past hundred years because of higher emissions of greenhouse gas resulting from anthropogenic impacts (WMO, 2017; Omar *et al.,* 2021).

The change in surface temperature and rainfall leads to an increasing water shortage, soil degradation, and reduction in crop yields (Ma *et al.,* 2018). Salinity significantly affects soil quality, vegetation growth (Perri *et al.,* 2018), and the yield of crops (Wang *et al.,* 2021). Among the strategic crops in Egypt, the yields of wheat are expected to be decreased by 9% in 2030 and 20% in 2060 (Omar *et al.,* 2021). This is due to seawater seepage in the seashore parts of Egypt causing soil salinization and a decline in vegetation (Perri *et al.,* 2018; Omar *et al.,* 2021). One of the major limitations to agriculture sustainability is the threat of soil salinization. The salinity and alkalinity conditions of seashore areas provide an overview of the process dynamics that led to the imbalance of the soil system (Ma *et al.,* 2018). Soil salinization is the accumulation of dissolved salts within the soil layers of a pedon forming *salic* horizons at specific depths from the soil surface (Soil Science Division Staff, 2017). The salinization and its interactions in soil solution can alter the behavior of soil properties and cause different geotechnical problems in crop yield and the environment (Omar *et al.,* 2021). The change in the geotechnical behavior of soil is chiefly due to the types of clay minerals in soil pedons and the chemical composition of anions and cations in saline water. Soil salinization can be formed through various processes either natural or anthropogenic factors (Eswar *et al.,* 2021). These processes may be a result of the capillary rise of salty groundwater, sedimentation of salt minerals, unfavorable activities of agricultural management, and industrial practices (Wang *et al.,* 2021).

Salt-affected soils occupy an area of more than a billion ha (Mha) worldwide, particularly in Africa, Asia,

*Corresponding author e-mail: dr.elwandrc@gmail.com

and South America (Eswar *et al.,* 2021). This causes a reduction in water quality and a rise in soil salt concentrations and therefore a decline in crop yield and soil degradation (Ma *et al.,* 2018). Accordingly, monitoring salinity status is becoming increasingly significant to avoid the salinization processes in arid lands (Eswar *et al.,* 2021). Land deterioration is a process in which the current capability of soil changes into the incapability/unsuitability of soils to produce different crops under different uses (Mukhopadhyay *et al.,* 2021). This process resulted in a reduction in the soil capacity and fertility to meet the requirements of biomass, human beings, and livestock, and therefore, the healthy functioning of land-based ecosystems is degraded. The land degradation categories in the Egyptian ecosystem are waterlogging, soil salinity, water erosion, and compaction due to the water level rise of the Mediterranean Sea (Abdel-Kader, 2019). The degradation of dryland in semi-arid and arid zones is an extensive and severe threat to the livelihoods of the comprehensive environment and many people in developing countries particularly in Egypt (Abdel-Kader, 2019). It is assessed that more than 25% of desert land or drylands are previously degraded (Zhang *et al.,* 2021) and approximately twelve million hectares of land per year are degraded (Abdel-Kader, 2019).

The coastal erosion and sea-level rise may decrease the comparative surface elevation of agricultural land above sea level and boost the frequency of tide submergence, therefore water logging and soil salinity problems may be produced (Zhang *et al.,* 2021). The rise of sea level may be caused by anthropogenic factors or natural controllers. When the maximum rate of the last glacial process of about 1 mm/yr throughout the late Holocene age, the global levels of the sea have risen (Field *et al.,* 2014). This allowed the development of coastal salt marshes through the deposition of salt sediment underground and greater than the rise of sea-level processes (Ruiz-Fernàndez, 2018). The global warming process was accelerated due to the anthropogenic measures causing the rise of greenhouse gas emissions throughout the past two decades and therefore (Field *et al.,* 2014). Hundreds of millions of people who reside in lowlands at the coastal lines that are vulnerable to permanent flooding with seawater are at a risk due to the rise of sea levels by climate change (Field *et al.,* 2014). The adaptation to climate change hazards in the agricultural sector can be classified into three types of adaptation procedures which are incremental, systemic, and transformational actions (Kumar *et al.,* 2017). The farm system cannot be altered by incremental and systemic adaptations (Platt *et al.,* 2020). In contrast, the farm system and its location can be changed by transformation measures based on the intensity and degree of the agricultural limitations and climate stressors (Panda, 2018).

Ismailia governorate is positioned on a low site that has elevations above sea levels ranging from 1 up to 33 meters (Abdeen *et al.,* 2018). The Suez Canal divided the Ismailia governorate into Ismailia West and Ismailia East, as well as the surrounding desert was sandy plain and dunes (Younis *et al.,* 2021). Hence, most areas of the Ismailia governorate are located in the lowland positions which are usually covered by the sand sheet, gravel, eolian sands, and marshes, with certain scattered hills of sandstone and limestone on the eastern side of the Bitter Lakes (Younis *et al.,* 2021). The El-Timsah Lake, the Great Bitter Lake, and Suez Canal are the major seawater bodies situating the lowlands of Ismailia East (Abdeen *et al.,* 2018). In general, the study lands are covered by recent Quaternary gravel, sands, and clay lenses (Younis *et al.,* 2021).

The present study was conducted in the El-Amal area, Ismailia East as a model for the Suez Canal region of Egypt. It aimed at studying the impacts of seawater seepage from the New Suez Canal of Egypt on pedomorphological and physicochemical characteristics of the studied soils and identifying the main drivers of soil salinity and land deterioration in the study area with an emphasis on the best adaptations to agricultural limitations and climate stressors. This study is the first to address the interaction between seawater intrusion and soil salinity concerning climate change adaptations in Egypt.

MATERIALS AND METHODS

Study area and climate criteria

The study was conducted in 2020 on 285 Faddan in the El-Amal farm area, Ismailia East, Egypt (Fig. 1). The El-Amal study area is situated in the central portion of the Suez Canal Development Corridor. It is bounded by 32° 21' 41" - 32° 22' 43" east and 30° 30' 41" - 30° 31' 33" north (Fig. 1). It is located 2 km from the New Suez Canal. The area's surface altitude above sea level was <7–11 m. The study area was a cultivated farm with different crops and fruit trees from the previous years. Drip irrigation was used as an irrigation system in the current farm in the El-Amal study area. The irrigation water was sourced from the River Nile, which is of fine standards for irrigation (Fig. 2). Ismailia East region is affected by anthropogenic activities such as agricultural lands, military sites, power plants, tunnels, tourist villages, irrigation canals, pipelines, industrial centers, and new urbanization such as the New Ismailia city.

Egypt's climate varies considerably from hot and dry summers to cold and mild winters. Precipitation has different and irregular patterns and can occur in unpredictable ways (Yassen *et al.,* 2020). The annual mean values of rainfall are very low, with rainfall rates ranging from less than 250 mm in north Egypt to 5 mm in the southern portions of Upper Egypt. The highest values of surface temperatures increase annually, reaches 40°C–49°C during the summer months, particularly in Upper Egypt (Yassen *et al.,* 2020). The climate of Ismailia governorate is characterized by a long period of cold winter, an intermediate period with light rains, and warm summer with high humidity. The annual precipitation rate does not exceed 100 mm (Egyptian Meteorological Authority, 2020). The average air temperature ranges from 27°C to 43°C. The wind is dry from the northwest, with an annual rate of evaporation of more than 855 mm/year. The study area's local weather in the Suez Canal zone is noticeably semiarid to arid conditions (Egyptian Meteorological Authority, 2020). Yassen *et al.* (2020) studied the spatial and temporal changes in the reference evapotranspiration (ETo) and its climatic drivers by analyzing meteorological data from the previous 35 years (1983–2017) across Egypt's ecosystems to confront the negative effects of climate change. The spatial change of ETo has occurred and increased since the 1980s in the soils of deltaic plains in northern Egypt, including the Suez Canal region during the summer months of June to October. To combat the greatest evapotranspiration caused by climate change, the irrigation water requirements for summer crops should be recalculated and scheduled for Egypt's agricultural and water resource management (Yassen *et al.,* 2020). The study area is highly affected by climate change (Yassen *et al.,* 2020).

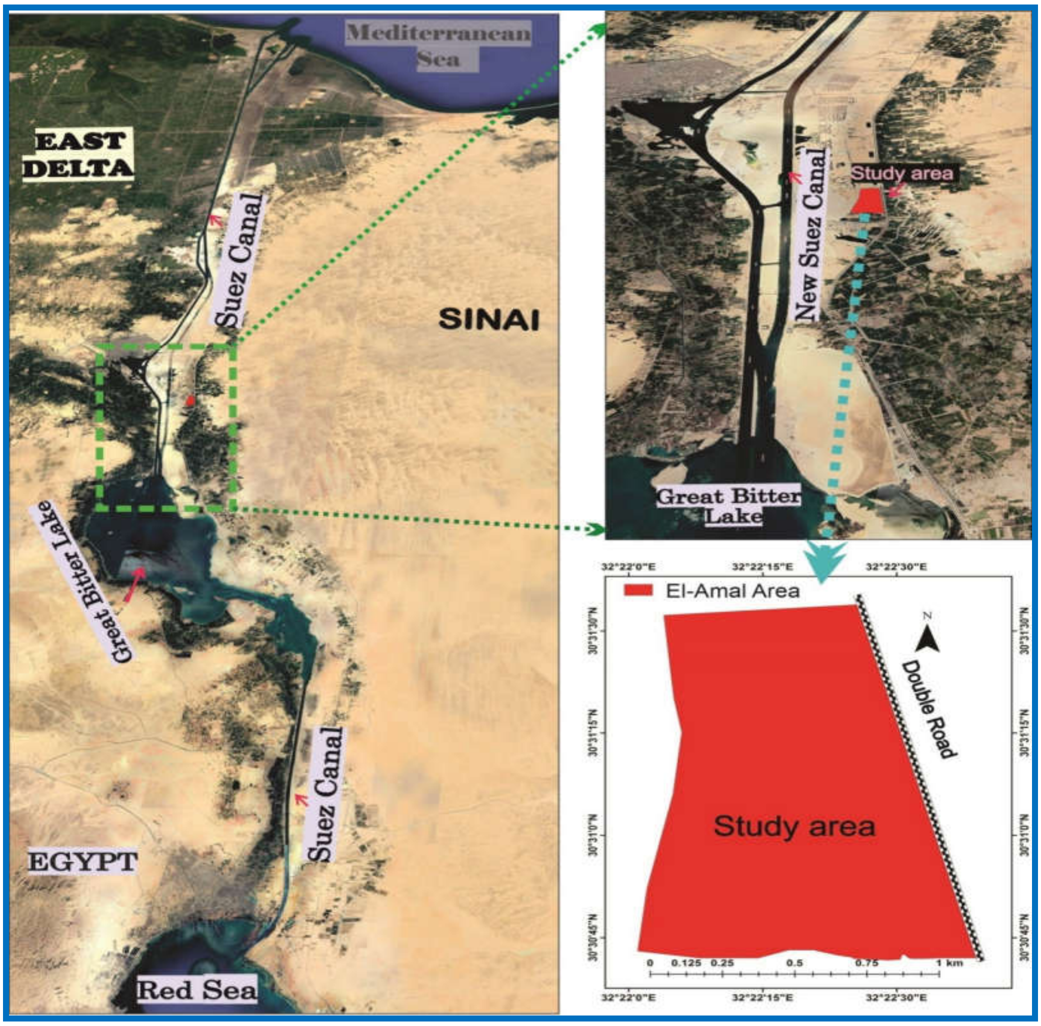

Fig. (1): Location of the El-Amal study area in Ismailia East, Egypt

Fig. (2): High-quality water was used for irrigating the study lands

Geomorphology and geology

The geomorphologic characteristics of the Ismailia East region, including the study area, significantly affect the shallow aquifer's hydraulic situations (Abdeen *et al.,* 2018). With the regular hydrogeology conditions across the investigation area being linked to the saltwater content in the underlying sand deposits (Abuzied *et al.,* 2020), the lowest elevations are situated in the inland lakes and the shallow water bodies that isolate the cultivated lowlands and sand sea (Hereher, 2018). Furthermore, groundwater beneath the study area is salty, with low recharge rates on the northern side of the study area (Hereher, 2018). The main sources of recharge for the shallow groundwater are the continuous seepage from the adjacent irrigated lands and the Suez Canal. The Suez Canal district faces a change in the groundwater table with the topographic slope (Hereher, 2018). The Suez Canal province corridor is located in a lowland area with elevations of less than 11 m above sea level (Abdeen *et al.,* 2018) (Fig. 3).

The regional geology of the study area was subjected to numerous investigations concerning the hydromorphological, geomorphological, and tectonic settings of the Suez Canal region (Abuzied *et al.,* 2020). The southwestern portion of the Suez Canal corridor is a part of a large tilted platform located in the north of Egypt (Ruiz-Fernàndez, 2018). The study area lands are covered with numerous formations (sedimentary rocks and sand depositions) from the Middle Miocene, Late Miocene, and recent Quaternary epochs (Fig. 3). The El-Shatt formation, dates back to the Middle Miocene and forms the eastern portion of the Bitter Lakes (Ruiz-Fernàndez, 2018). El-Shatt Formation consists of sandstone, mudstone, limestone, and gypsum. Whereas, the Hagul formation is from the Late Miocene (Abuzied *et al.,* 2020). The major sediments of the Hagul formation are the nonmarine sediments of gravel, flint pebbles, sands, occasionally sandy limestone, and sandstone. Furthermore, the recent formation of gravel (Gravelly plain), eolian sand, clay particles, wadi deposits, dunes, sabkhas, and salt marshes are the components of the Quaternary age that covers most study lands (Abdeen *et al.,* 2018; Ruiz-Fernàndez, 2018) (Fig. 3).

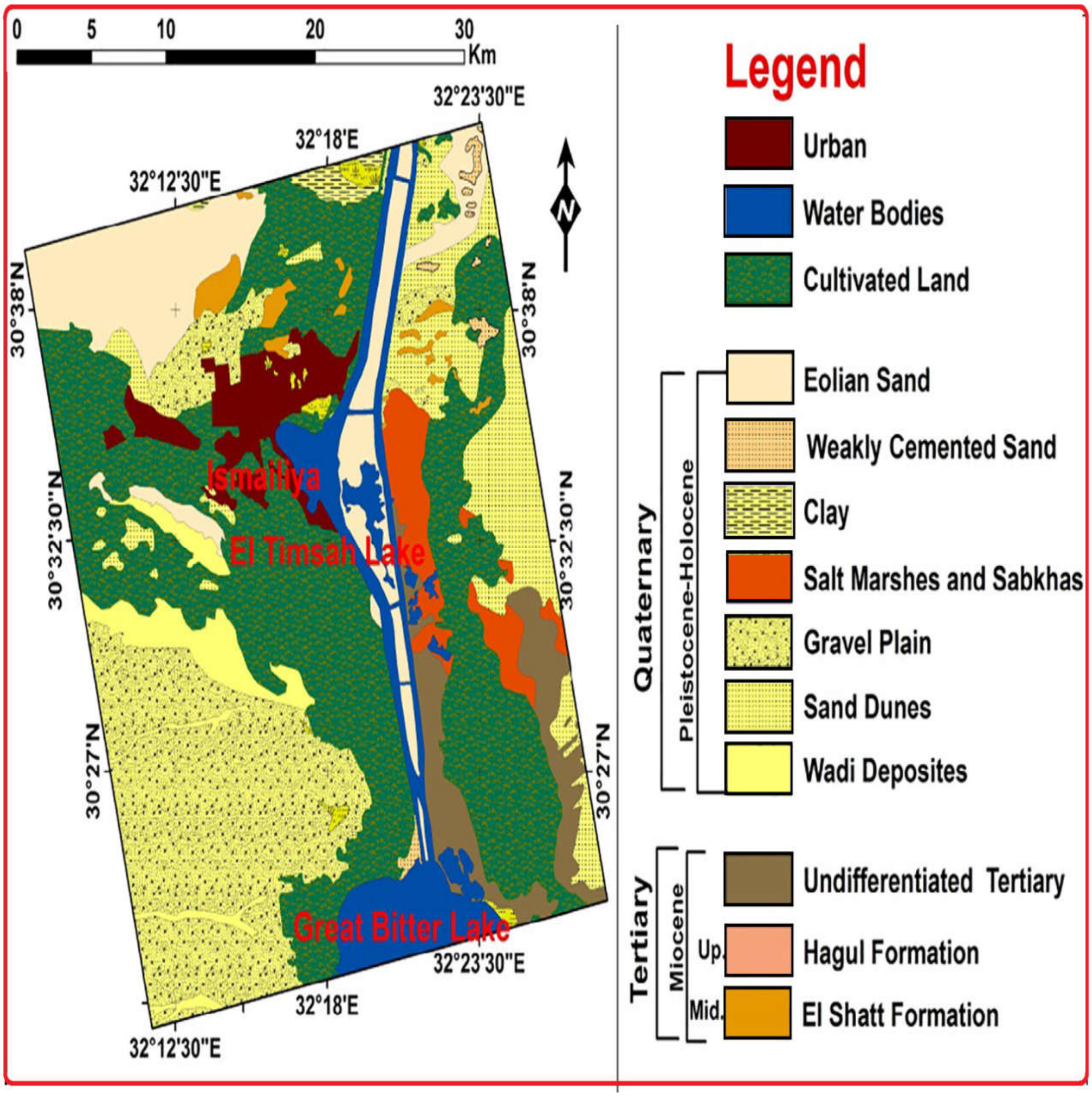

Fig. (3): Simplified geological map of the Suez Canal region including the study area (modified after Abdeen *et al.,* 2018)

Fieldwork, laboratory methods, and data processing

Nineteen soil pedons were regularly distributed over 285 Faddan in the El-Amal area as a grid system to achieve a detailed soil survey representing the variation intensity over the study area. Among the soil pedons studied, the analysis data for only twelve pedons are presented in Tables (1 and 2) as representative ones in the current work. The morphological description of layers and horizons of the study soil pedons as well as their positions were conducted in the farm field using the standard methods recommended by FAO (2006) and the Soil Science Division Staff (2017). The global positioning system device was used to locate each georeferenced soil pedon in the field. The collected soil samples from each soil pedon were transferred to the laboratory for the required analysis. Soils were air-dried and separated from the coarse earth fraction by sieving. The prepared and separated soil was bagged and stored for further laboratory analysis. The soil textural composition, the coarse fraction (gravel), soil pHe of saturated paste, exchangeable sodium percentage (ESP), electrical conductivity (ECe), and lime (CaCO3) were estimated following the standard procedures given by the Soil Survey Staff (2014). Furthermore, seven water samples were collected from the water table observed within the study pedons at different depths. The pHw and ECw (dS/m) of water table samples were measured according to Ayres and Westcott, (1976) and Clesceri *et al.* (1998). The soil suitability analysis was performed using the standard methods recommended by FAO (1976; 2007) and Elwan (2013; 2019). The geostatistical processing of the obtained results was managed and performed with the ArcGIS 10.1 software (ESRI, Redlands, CA) to generate various thematic maps. The obtained maps were thus assembled to create categorical maps.

RESULTS AND DISCUSSION

Mapping and characterization of the study soils

A detailed soil survey was conducted, and pedomorphological observations of soils were registered in the field and are presented in Table (1). Furthermore, the analyzed physical and chemical characteristics of soils, and the chemical properties of water table samples are presented in Tables (1 and 2). The entire soil occupied an area of 285 Faddan. In contrast to sabkha lands, soils in the study area were classified into five soil mapping units (SMUs) (Fig. 4) based on effective soil depth, textural class, soil salinity, and depth of the water table depth (Figs. 4–10). The first three units (67.8 Faddan; 23.8%) were deep: SMU1 for deep, sandy, nonsaline soils with no water table at 150 cm (Fig. 5), SMU2 for deep, sandy, slightly saline soils with a hardpan (Fig. 6), and SMU3 for deep, sandy, moderately saline soils with a water table at 105 cm (Fig. 7). Whereas the other two units were moderately deep to shallow soils, with SMU4 for moderately deep, sandy, strongly saline soils with a water table of 50–100 cm (Fig. 8) and SMU5 for shallow, sandy, strongly saline soils with a water table of less than 50 cm (Fig. 9). Investigated soils were grouped into three classes; deep (67.8 Faddan; 23.8%), moderately deep (48.8 Faddan; 17.1%), and shallow (123 Faddan; 43.2%) soils based on the depth of the regolith. Furthermore, an area of 45.4 Faddan (15.9%) was made up of scattered sabkhas and salt marshes that were severely affected by seawater intrusion (Fig. 10). The soils of SMU 1 and SMU2 have surface elevations of 9–11 m above sea level meanwhile the soils of SMU3, SMU4, and SMU5 have altitudes of 7–8 m above sea level. conversely, the sabkha area was elevated by more than 7 m above sea level.

The soil color of all pedons varied slightly from gray 10YR (5/1) to brown (7.5YR 4/2, 4/4). Under saturation conditions, the soil color darkens. The soils of the study area widely ranged from well drained to very poorly drained soils (saturated soils) (Table 1). The entire pedons of saturated soils exhibited structureless units (e.g., single grain or massive) throughout the pedon layers compared to the granular and subangular blocky structures that dominated the drained soils in SMU1 and SMU 2. The soil structure may be destroyed under flooded conditions with seawater. The wet consistency was observed in the field to be nonplastic to slightly plastic and nonsticky to slightly sticky due to the coarse texture. Many pedological and redoximorphic features, as well as finely disseminated salt crystals and manganese films, were observed in the saturated soils under study, serving as indicators of the periodic saturation of the lower parts of the pedon. Iron was oxidized mostly on drained soil surfaces and reduced in saturated soils. Carbonate features were observed in the form of few to common nodules, concretions, and masses, particularly in well-drained soils. The gravel content ranged from none in the shallower pedons to 12.28% in deeper soils (Figs. 5–10.(

The entire soil texture group is a sandy soil material and, with a subgroup of coarse-textured soils. The percentage of sand in the soil ranged from 97.20% to 99.89%. Conversely, the finer fractions (silt plus clay) were discovered to be less than 3% in the investigated soils. The water table existed at various positions and depths in the soil pedons. Soils in SMU 4 and SMU 5 were heavily influenced by a higher water table at 50–100 cm and below 50 cm, respectively, whereas soils in SMU 3 were characterized by a lower water table at a depth of 105 cm from the soil surface. In contrast, the water table was absent in the deep soils of SMU 1 and SMU 2.

Soils in the study area reflected the extensive variation in soil reaction: from neutral to strongly alkaline. Most of the area is moderately alkaline to near neutral reaction. The values of ESP widely varied from 2.48% in SMU 1's drained soils to 27.15% in SMU 5's saturated soils. The increased values (>15%) in the study soils indicate sodium hazards in the soils. The electrical conductivities (EC) of the study soils widely varied from nonsaline (EC < 2 dS/m) in SMU 1 to strongly saline (EC > 16 dS/m) in SMU 3 and SMU 4. Most study soils that have high EC values (171.8 Faddan; 60.3%) were found in a strong saline zone (16.65–29.60 dS/m). In soils of SMU 3, EC values ranging from 9.73 to 11.500 dS/m were found in the lower and upper layers of the same pedon, respectively.

These areas must either implement adaptation measures or adopt salt-tolerant crops and land-use changes. With the alkalinization may be being caused by the accumulation of sodium carbonates (Na_2CO_3) sourced from the study area's direct Suez Canal facing location, seawater intrusion, and seepage of brackish water into the soil, higher soil salinization might also be caused by the intrusion of saline water from the New Suez Canal.

Table (1): Certain pedomorphological and physical characteristics of study soils

Soil pedon	Depth (cm)	Gravel (%)	Soil Morphology			Textural Composition[§] (%)			
			Drainage	Features[Љ]	Structure[¥]	CS	FS	Si + C	Texture
SMU 1: Deep, sandy, nonsaline soils with no water table at 150 cm (Drained soils)									
1	0–25	9.09	Well-drained	F3M, CAN	2, GR	36.84	62.00	1.16	Fine sand
	25–60	6.67		F3M, FED, CAM	0, MA	46.07	52.54	1.39	Fine sand
	60–90	12.28		F3M, CAN	1, GR	54.51	44.17	1.32	Coarse sand
	90–135	2.31		CAM, CAN	0, MA	42.72	56.17	1.11	Fine sand
2	0–30	0.88	Moderately well-drained	CAN, FMC	3, SBK	29.43	69.21	1.36	Fine sand
	30–65	0.00		FMC, FMN	0, SGR	81.63	18.20	0.17	Coarse sand
	65–125	0.00		F3M, CAN, CAM	2, GR	23.14	76.74	0.12	Fine sand
3	0–50	4.44	Somewhat poorly drained	F3M, CAM	1, GR	73.27	24.42	2.31	Coarse sand
	50–100	0.00		F3M, FED	0, SGR	27.16	72.34	0.50	Fine sand
	100–120	8.62		F3M, CAM	2, SBK	23.27	76.3	0.43	Fine sand
4	0–25	0.00	Moderately well drained	F3M, CAC	1, GR	78.37	20.72	0.91	Coarse sand
	25–80	0.00		F3M, FED	0, MA	16.28	83.01	0.71	Fine sand
	80–130	0.00		None	0, MA	76.31	23.27	0.42	Coarse sand
SMU 2: Deep slightly saline and slightly calcareous sandy soils with a hardpan									
5	0–40	1.08	Somewhat poorly drained	F3M, CAM	1, GR	77.74	21.84	0.42	Coarse sand
	40–85	0.00		F3M, CAC	0, MA	22.78	76.45	0.77	Fine sand
	85–110	0.00		F3M, FED	3, SBK	37.60	61.80	0.60	Fine sand
	110+	Extremely calcareous hard layer with weathered limestone fragments.							
SMU 3: Deep, sandy, moderately saline soils with a water table at 105 cm									
6	0–20	0.00	Somewhat poorly drained	FDS, RMX, F2M	0, MA	19.72	79.65	0.63	Fine sand
	20–50	0.00		SIC, RMX, F2M	0, SGR	28.68	71.09	0.23	Fine sand
	50–90	0.00		SAX, FMC, FMN	0, SGR	80.85	18.58	0.57	Coarse sand
	90–105	0.00		FDS, RMX, FMC	0, MA	15.3	83.69	1.01	Fine sand
	105+	Water table level							
SMU 4: Moderately deep, sandy, strongly saline soils with a water table of 50 – 100 cm									
7	0–40	0.00	Poorly drained	SIC, FDS, F2M	0, MA	8.36	88.84	2.80	Fine sand
	40–90	0.00		FDS, RMX, F2M	0, SGR	16.89	82.76	0.35	Fine sand
	90+	Water table level							
8	0–30	0.95	Poorly drained	FDS, RMX, F2M	0, MA	70.23	29.58	0.19	Coarse sand
	30–70	5.00		FDS, RMX, FMC	0, SGR	66.71	31.83	1.46	Coarse sand
	70+	Water table level							
9	0–20	0.00	Very poorly drained	FDS, RMX, F2M	0, SGR	60.00	39.15	0.85	Coarse sand
	20–55	0.00		FDS, SAX, F2M	0, MA	83.13	16.17	0.70	Coarse sand
	55+	Water table level							
SMU 5: Shallow, sandy, strongly saline soils with a water table below 50 cm (Saturated soils)									
10	0–15	4.24	Very poorly drained	FDS, RMX, F2M	0, SGR	70.11	28.3	1.59	Coarse sand
	15–45	0.00		FDS, SAX RMX	0, SGR	19.25	80.32	0.43	Fine sand
	45 +	Water table level							
11	0–14	0.00	Very poorly drained	FDS, RMX, F2M	0, SGR	54.78	45.11	0.11	Coarse sand
	15–40	5.56		FDS, RMX, F2M	0, MA	37.42	62.05	0.53	Fine sand
	40+	Water table level							
12	20	0.00	V. poorly drained	FDS, RMX, F2M	0, SGR	26.75	72.92	0.33	Fine sand
	20+	Water table level							

Explanation: [Љ]***Pedological features:*** **RMX** (reduced matrix); **F2M** (reduced iron, Fe^{+2}, masses); **F3M** (oxidized iron, Fe^{+3}, masses); **FMC** (iron-manganese concretions; cemented distinct layer); **FMN** (iron-manganese nodules, cemented); **FED** (iron depletions); **FDS** (finely disseminated salts); **SAX** (salt crystals); **CAM** (carbonate masses); **CAN** ($CaCO_3$ nodules); **CAC** (carbonate concretions in matrix); **SIC** (Silica concretions). [¥] ***Soil structure:*** **0** (structureless); **1** (weak); **2** (moderate); **3** (strong); **SBK** (subangular blocky); **GR** (granular); **SGR** (single grain); **MA** (massive). [§] **CS** (Coarse sand); **FS** (Fine sand); **Si** (Silt); **C** (Clay).

Table (2): Selected chemical properties of soil mapping units and water table samples

Pedon	Depth (cm)	Soil parameters				Water table	
		$CaCO_3$ %	pH_e	ESP (%)	EC_e (dS/m)	pH_w	EC_w (dS/m)
SMU 1: Deep, sandy, nonsaline soils with no water table at 150 cm (Drained soils)							
1	0–25	3.84	8.44	14.25	0.70	--	--
	25–60	2.99	8.19	13.54	0.52	--	--
	60–90	4.27	7.95	10.25	1.30	--	--
	90–135	4.69	7.67	10.36	1.10	--	--
2	0–30	6.57	7.40	3.15	0.66	--	--
	30–65	2.56	7.55	6.45	0.69	--	--
	65–125	3.07	7.35	2.48	0.96	--	--
3	0–50	3.75	7.49	6.35	1.75	--	--
	50–100	3.41	8.53	1125	0.74	--	--
	100–120	3.58	8.12	13.65	0.65	--	--
4	0–25	1.89	7.81	8.45	1.00	--	--
	25–80	2.05	7.85	7.65	1.95	--	--
	80–130	2.90	8.09	4.19	1.30	--	--
SMU 2: Deep slightly saline and slightly calcareous sandy soils with a hardpan							
5	0–40	3.41	8.16	14.15	3.70	--	--
	40–85	2.56	8.05	11.05	6.30	--	--
	85–110	35.83	8.39	13.65	3.22	--	--
	110+	Extremely calcareous hard					
SMU 3: Deep, sandy, moderately saline soils with a water table at 105 cm							
6	0–20	1.71	7.85	17.15	11.50	--	--
	20–50	1.37	7.95	18.34	10.90	--	--
	50–90	3.41	8.38	19.34	8.30	--	--
	90–105	2.99	8.13	21.45	9.73	--	--
	105+	Depth to water table level				7.89	16.15
SMU 4: Moderately deep, sandy, strongly saline soils with a water table of 50 – 100 cm							
7	0–40	4.78	8.58	21.58	26.00	--	--
	40–90	3.58	8.85	18.34	17.50	--	--
	90+	Depth to water table level				8.17	19.33
8	0–40	2.30	8.95	19.45	19.95	--	--
	40–65	1.11	8.57	23.15	16.65	--	--
	65+	Water table level				8.31	12.35
9	0–20	3.16	8.26	24.05	21.39	--	--
	20–55	2.90	8.70	25.15	17.56	--	--
	55+	Depth to water table level				8.11	15.53
SMU 5: Shallow, sandy, strongly saline soils with a water table below 50 cm (Saturated soils)							
10	0–15	5.38	8.59	22.15	29.60	--	--
	15–45	0.85	8.75	23.45	17.60	--	--
	45 +	Depth to water table level				7.98	21.08
11	0–15	2.99	8.99	19.45	22.10	--	--
	15–40	1.71	8.87	20.65	19.22	--	--
	40+	Depth to water table level				7.65	17.50
12	20	6.40	8.95	27.15	23.13	--	--
	20+	Depth to water table level				7.84	11.55

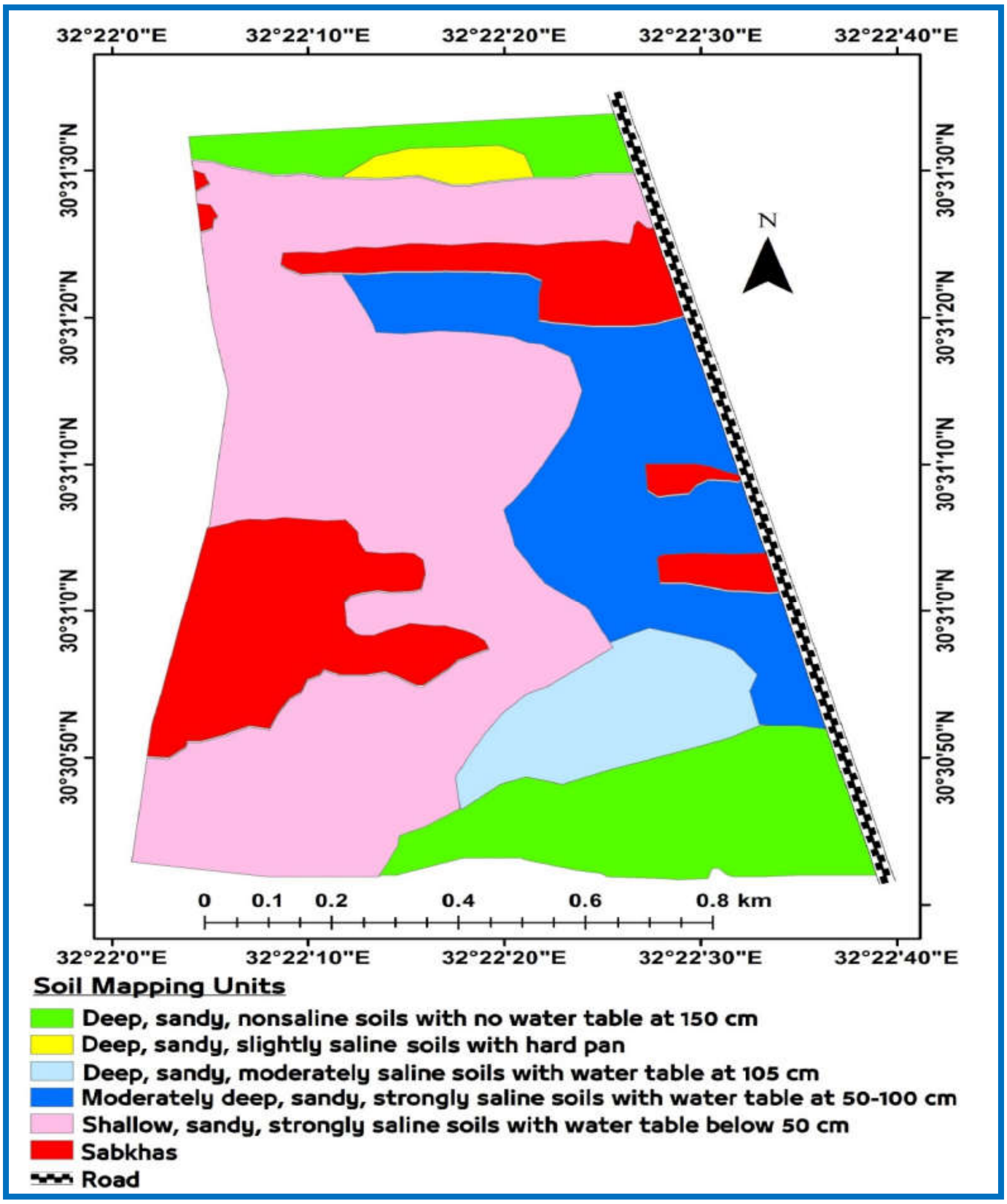

Fig. (4): Soil mapping units of the study area

Fig. (5): Site topography and pedon description of nonsaline soils in the first soil mapping unit (SMU 1)

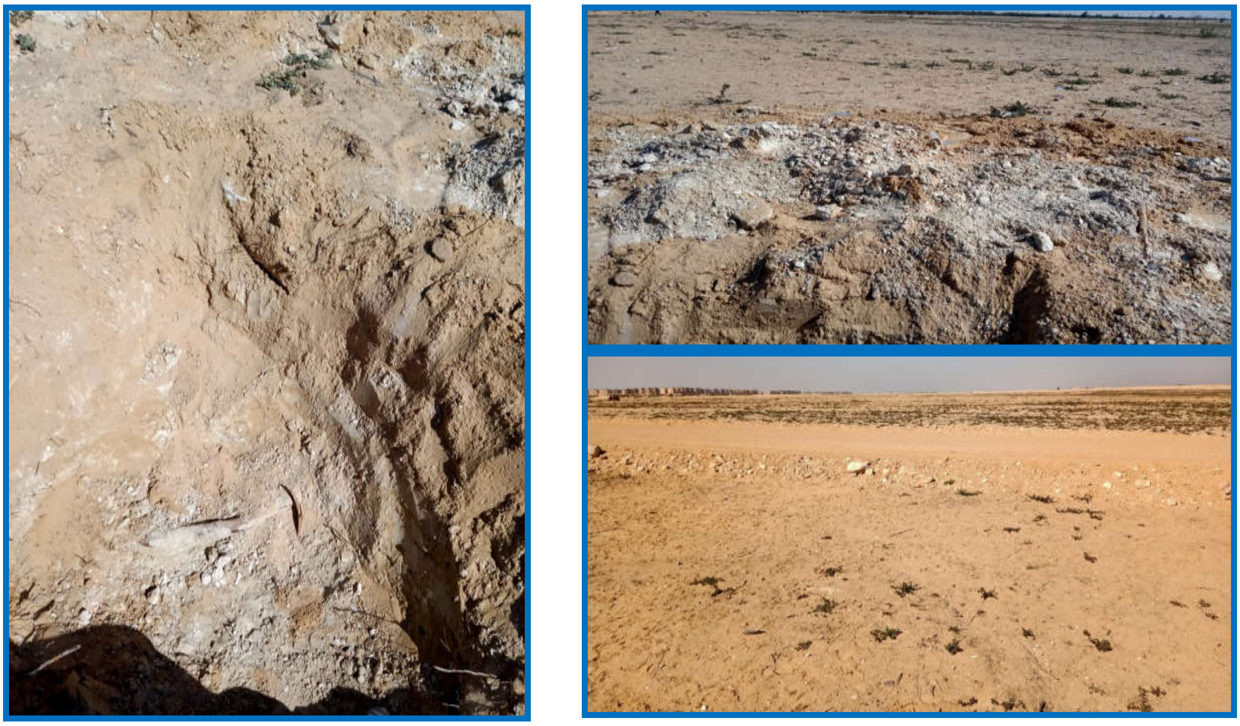

Fig. (6): The site and pedon descriptions of deep soils with hardpan in SMU 2

Fig. (7): The site and pedon descriptions of saturated soils at 105 cm in SMU 3

Fig. (8): The wilted and dead trees at the site with pedon activities of saturated soils at 50–100 cm in SMU 4

Fig. (9): The wetness site surface with pedon activities of fully saturated soils below 50 cm in SMU 5

Fig. (10): The inundation of soil surface and pedon layers and producing sabkhas and salt marshes in the lowlands

Soil suitability of the study area

The suitability and potentiality analysis of study soils were determined through scientific integration of different criteria of soil, irrigation water, and climate based on weights and scoring for each criterion using the standard procedures given by FAO (1976; 2007) and Elwan (2013; 2019). Briefly, the entire soils of the study area were classified into three suitability classes (moderate, marginal, and unsuitable) based on their suitability for cultivation (Fig. 11). The moderately suitable soils cover an area of 48.3 Faddan, whereas, the marginally suitable soils occupy an area of 19.5 Faddan. Most of the study lands (217.2 Faddan; 76.2%) were classified as unsuitable (Fig. 11). Approximately 23.8% (67.8 Faddan) of the study area was determined to be moderate to marginally suitable for cultivation. Many crops grow well in slightly saline soils and the expected productivity is also relatively higher in soils of SMU 1 and SMU 2 than in soils of SMU 4 and SMU 5.

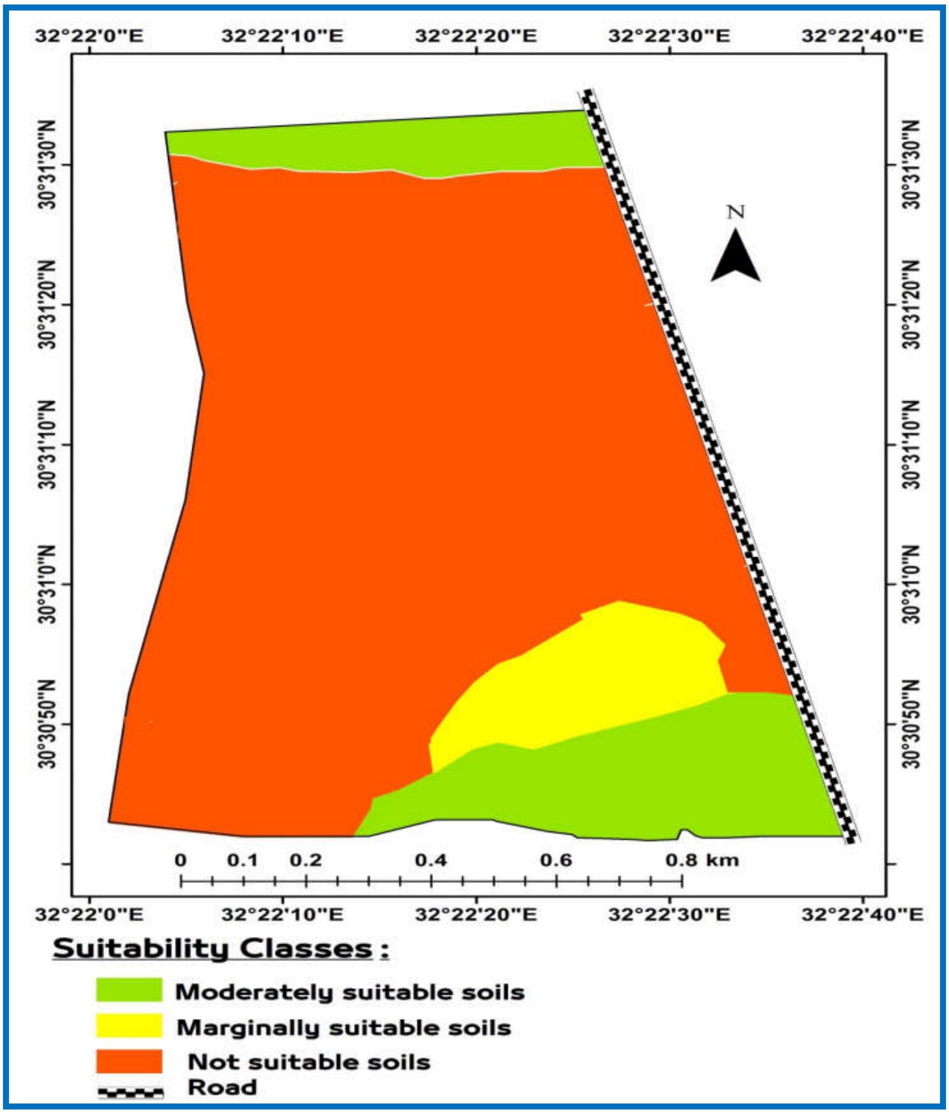

Fig. (11): Soil suitability classes in the study area

Rising water table across the study soils

The morphology observations of the water table emergence within the study soil pedons were studied in the field. The internal pores and spaces between soil particles were completely saturated with groundwater seepage from the Suez Canal, with the identified water table being defined as the separated boundary between the underground-saturated zone and the unsaturated zones within the study pedons. The most studied soils lack natural drainage which is described by the Soil Science Division Staff (2017). The soil morphology and water regime were changed under the permanent saturation conditions caused by the continuous seawater seepage in the study soils. Under saturation conditions, the study soils of saturated SMUs (shallow soils) had a peraquic soil moisture regime. Furthermore, the salinity (ECw) of the study water table varied from 11.55 dS/m (moderately saline) to 21.08 dS/m (strongly saline) (Table 2). In the saturated soils at SMU4 and SMU5, water is slowly removed and the soil is wet for long periods at shallow depths. The internal free water occurred at depths ranging from shallow to very shallow. Most cultivated crops cannot be grown under free water conditions for an extended period during the growing season of trees, the soil cannot be artificially drained, causing them to wilt and die (Figs. 8 and 9). Free water at shallow depths was common and abundant in saturated SMUs. In the sabkha lands, the soil pedons were fully saturated with free water above the soil surface (Fig. 10). The internal free water within pedon layers caused by seawater seepage was permanent for more than 21 h per day. The results showed that the water table was raised to 105 cm from the soil surface in the saturated soil of SMU3, whereas it was significantly raised to 100–<50 cm in moderately deep and shallow soils of SMU4 and SMU5, respectively. In contrast, the soil was highly drained in SMU1 and moderately drained in SMU2. The saturated conditions of waterlogging and soil salinization can reduce soil quality and crop yield productivity (Zhang *et al.,* 2021), where aspects contributing to excessive Na_2CO_3 salt accumulation and humus decomposition as observed in the studied soil (Figs. 12, 13, and 14) being linked to seawater seepage, which is caused by the rising level of seawater (Rahman *et al.,* 2018). These conditions can negatively affect the quality of groundwater when used for irrigation (Omar *et al.,* 2021).

Impacts on soil properties

The properties of investigated soils were degraded by different processes induced by the seepage of seawater from the New Suez Canal. With primary salinization and salt accumulation in the study soils being caused by natural processes due to high salt groundwater translocated from the Suez Canal, the lands between the Suez Canal and the area under study are predominantly saturated with brackish seawater resulting in seepage of saline water into the soil layers of the investigated area. This resulted in alkalinity and salinity across vertically soil pedons (Table 2). Furthermore, secondary salinization can be caused by human interventions as anthropogenic effects such as the mismanagement of irrigation and fertilization under insufficient or poor drainage (Zhang *et al.,* 2021). However, the current study found that the quality of irrigation water provided by the Nile River was good (Fig. 2). The global climate change is another contributor to land degradation (Wang *et al.,* 2021), as a consequence of the irrigation system used in the farm of El-Amal area being the drip method as a new technique for water management, with the soils being degraded and the infrastructure of the drip system destroyed due to high levels of soil salinity (Fig. 12). The accumulation of sodium salts caused by seawater intrusion is one of the main physiological challenges confronting the affected soils (Fig. 13). Salts from seawater can harm plant growth and development by interfering with nutrient uptake by plants under salinity stress (Mukhopadhyay *et al.,* 2021). Furthermore, saturation conditions reduce the oxygen level in the soils, restricting plant respiration (Martínkovà *et al.,* 2021), resulting in reduced growth and yield (Eswar *et al.,* 2021).

Fig. (12): Destruction of the drip irrigation network due to the desertification of the study soils

Fig. (13): White salt crust (NaCl) and growth only the tolerant desert shrubs and withering other desert grasses across the saturated soil in SMU 3, SMU 4, and SMU 5

Attributed to the soil structure which was destroyed in sodic-saline soils and consequently, making them more susceptible to soil deterioration, the salinization process was prevalent in SMU 4 and SMU 5 soils, decreasing soil quality and vegetation cover in these soils (Figs. 8, 9, 12, and 13). As illustrated in Figs. (12 and 13), land degradation extensively occurred in the study soils and caused soil desertification. The salinization process promotes the degradation of soil morphology, physical, chemical, and microbiological properties (Naylor *et al.,* 2021), resulting in soil desertification (Abdel-Kader, 2019). In Egypt, salinization is a major challenge due to rising temperatures and decreased rainfall caused by climate change (Zhang *et al.,* 2021).

The anaerobic conditions of the study salinity-stressed soils negatively affect the metabolism of the microorganisms in the soil, causing a decline in both soil fertility and thus crop yield (Naylor *et al.,* 2021; Shalby *et al.,* 2021). With an excess of sodium cations in the soil solution leading to the degradation of soil morphology and physical properties, high salinity levels in soils under saturation conditions cause withering of vegetation due to the increase in osmotic pressure effects of NaCl salts (Figs. 13; 14). The sodium salts degrade the soil structure and aggregates, reducing the oxygen rate in the soil (Martínkovà *et al.,* 2021) (Figs. 13 and 14). Soil salinization augmented the impermeability of deep sandy soil layers and resulted in permanent poor drainage (Zhang *et al.,* 2021). This makes the soil unsuitable for plant growth and cultivation (Figs. 7, 8, and 9).

Fig. (14): Decaying of humus and withering of desert shrubs due to the surface salt crust of Na_2CO_3

Responsible drivers of soil salinization and climate change adaptations

Climate change is considered a major dynamic contributor to soil salinity alterations in the arid desert ecosystem of the El-Amal area in Egypt's Suez Canal region (Fig. 15). The main parameters of climate change, in this case, are the rise in temperature and seawater level as well as variation in rainfall patterns (Fig. 13). And, with the annual rainfall of Egypt being less than 250 mm, compared to a global average value of 860 mm (Eswar *et al.,* 2021), the combination of the above parameters can decrease or increase water resources, resulting in drought or flash flooding, respectively, both of which are considered key elements causing full soil salinization and land deterioration (Fig. 15). In the El-Amal study area, the recharge of groundwater may be negatively impacted by variability in both rainfall and temperature under climate change impacts. Therefore, with the water table in the study soil pedons rising to inundate the lowland, forming sabkha and salt marshes (Ruiz-Fernàndez, 2018) (Figs. 10 and 15). the soil salinity in the current study area was caused by the intrusion and seepage of the saltwater into the study lands, and therefore. Numerous studies have been conducted globally to examine the relationship between soil salinization and climate change variables. For instance, Rahman *et al.* (2018) studied the shift in soil salinization from nonsaline to strongly saline along the coastal lines of Bangladesh over a 25 yr period from 1990 to 2015. They stated that the change in soil salinity in Bangladesh was due to the rise in sea level from 7007 mm in 1983 to 7129 mm in 2003 on the coast of Bangladesh. A rise in sea level in this area is predicted to further increase to flooding the whole land causing further salinization (Rahman *et al.,* 2018).

There are many drivers for soil salinization within the study land in the Suez Canal region. These drivers may be caused by climate change. There are numerous and should be carefully studied to fully understand the salinized soils of coastal areas. Augmented temperatures and differing rainfall patterns have posed a threat to the availability of soil and water resources. Additionally, the salinity of arid soils worldwide has resulted in both alterations in the dynamics of organic carbon storage under the impact of sea-level rise (Ruiz-Fernàndez, 2018), the population of soil microbes, and nitrogen cycling in saline flooding (Naylor *et al.,* 2021), and enzyme activity of a saline soil from the Yellow River delta in China (Zhang *et al.,* 2021).

The rise of mean sea level is a worldwide phenomenon of land degradation on coastlines and lands around the world due to global warming, which can raise the sea levels by 0.29–1.1 m at the end of the current century (Pörtner *et al.,* 2019). Globally, the glacial ice melting and water thermal expansion in seas and oceans are the universal causes of sea-level rise (Hoover *et al.,* 2017). The study land is shifting from suitable to unsuitable lands due to these global processes, which are linked to the increase in seawater seepage into groundwater, raising the water table of the affected lands. The surface temperature of the earth is another driver for soil salinization, which is directly linked to anthropogenic greenhouse gas emissions (Zhang *et al.,* 2021). The global climate will gradually change, with an average temperature rise of 4.8°C at the end of the 21st century (Perri *et al.,* 2018).

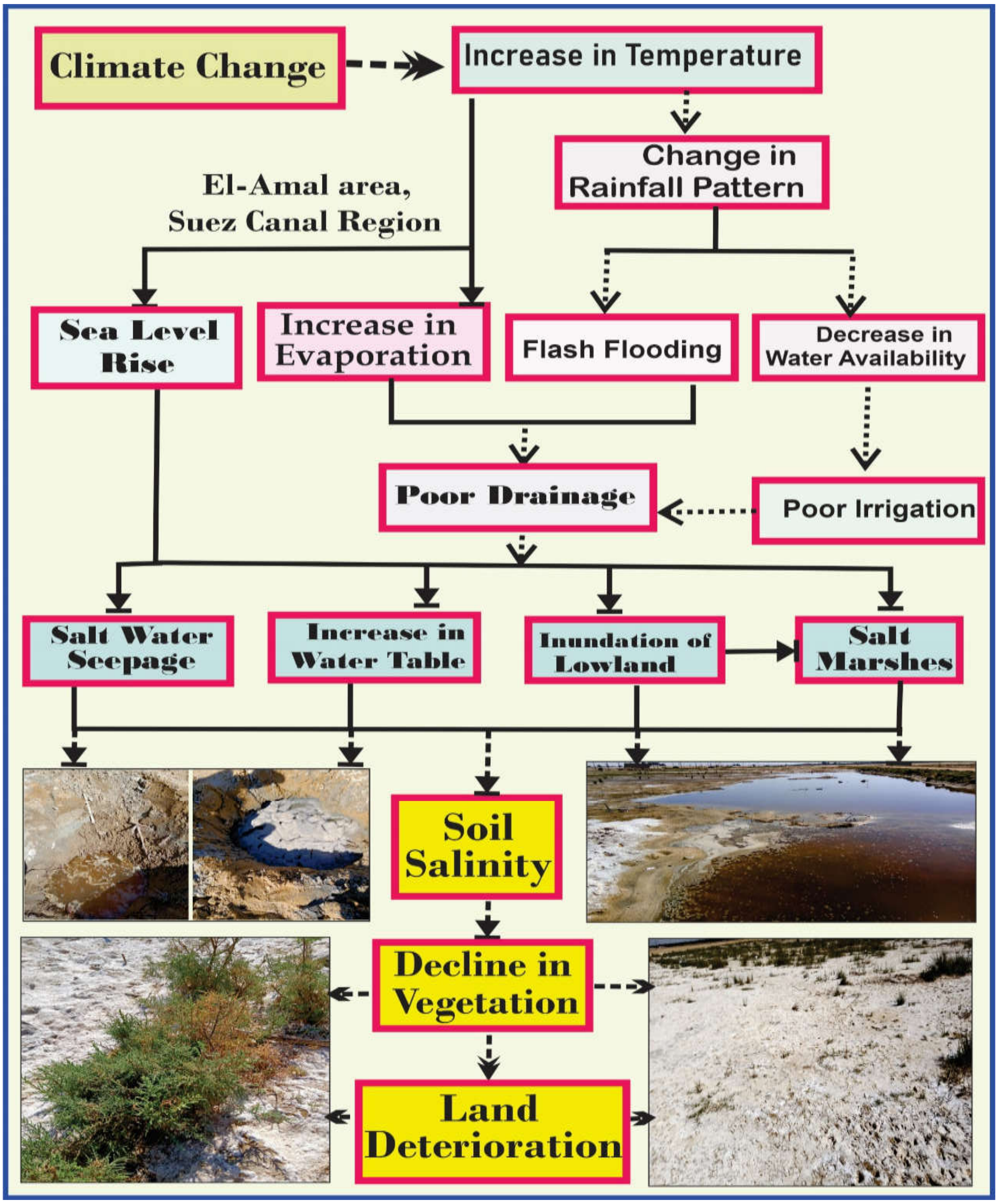

Fig. (15): Soil salinity and land deterioration diagram affected by climate change in the study area along the Suez Canal region of Egypt

Soil crust, rising water table, and declining vegetation were the most frequent field observations in the study area. It is predicted that the seepage of saltwater from the New Suez Canal will increase salinization in the adjacent coastal regions. The decline in vegetation cover was due to the high salinity caused by saltwater seepage that alters the groundwater table equilibrium and contributes to soil salinization (Perri *et al.,* 2018). Furthermore, with the salt accumulation on the soil surface as the salt crust (Figs. 13, 14, and 15) occurring when the saline water table is lost by evaporation through capillary action, and the salts not being leached through internal drainage into the sublayers within soil pedon and extreme evaporation, continuous irrigation under saline conditions and poor soil drainage is linked to soil salinization. Ultimately, the soils of SMU 3, SMU 4, and SMU 5 were highly impacted by seawater seepage, fully saturated, and degraded because their altitudes were 7–8 m above sea level, whereas drained soils of SMU 1 and SMU 2 had elevations of 9–100 m above sea level. In contrast, the soils less than 7 m above sea level were converted to salt marshes and sabkhas. Accordingly, it is predicted that the soils of SMU 1 and SMU 2 and other adjacent lands (3 km from the New Suez Canal) will be shifted into desertified lands in the future by continuous seawater seepage due to global climate change unless all protective strategies and adaptation measures are taken (Kumar *et al.,* 2017; Panda, 2018; Platt *et al.,* 2020). The adaptation measures to climate change in the agricultural sector may be related to incremental, systemic, and transformational changes (Panda, 2018), as shown in Fig. (16). The transformational adaptation of agricultural systems to the following stressors in the current study lands is more suitable and effective than incremental and systemic actions, with the study area experiencing very severe limitations and stressors to soil salinization and drought due to seawater seepage and climate change. Accordingly, transformational actions should be taken first, then the other two types of adaptation practices (incremental and systemic) should be followed appropriately (Fig. 16).

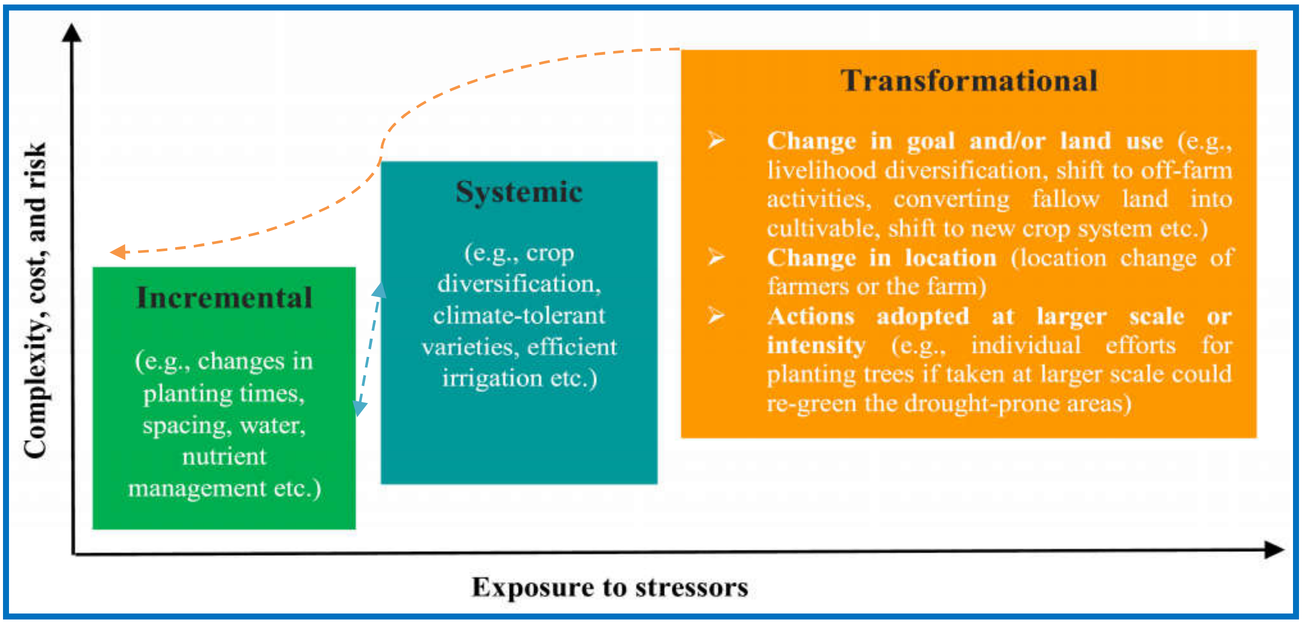

Fig. (16): Adaptation actions should be followed in the currently studied farmlands to combat the agricultural limitations and climate change stressors

CONCLUSIONS

The impacts of seawater seepage on characteristics of 285 Faddan at the El-Amal area of East Ismailia were studied. The selected area was investigated as a soil model for agricultural lands in the coastal zones of the Suez Canal corridor in Egypt. The elevations of the studied lands were registered between less than 7 and 11m above sea level. Five soil mapping units were identified in the studied farm. The soils varied from deep to shallow soil pedons. The majority of studied soils were moderately deep to shallow soils with the rise of a water table at 50 to 100 cm due to seawater intrusion. The shallow soils were highly affected by seawater seepage and soil salinization because of rising levels of the water table within the upper 50 cm of the soil pedon. Approximately 45.4 Faddan were recognized as scattered sabkhas and salt marshes in the study area due to the heavy seepage of seawater. With the majority of study soils (217.2 Faddan; 76.2% of the total area) being identified as unsuitable soils due to the high limitations of soil salinization, alkalinization, soil depth, and poor drainage, the study soils were tested for suitability. The soil salinity reached 29.60 dS/m in the saturated soils, posing a significant challenge to agriculture in the area. The study concluded that the morphological, physical, and chemical characteristics of 76.2% of the total area were degraded and converted into unsuitable lands for cultivation due to high salinity, which is linked to seawater seepage and thus raising the water table of the concerned lands. It is also predicted that the degradation of the soils of SMU 1 and SMU 2 may occur in the future because of continuous seawater seepage from the New Suez Canal caused by climate change. Furthermore, sustainable coastal planning for agriculture and irrigation projects in Egypt should be further investigated to control future climate changes.

In this context, decreased rainfall, erratic rainfall patterns, temperature warming, and sea-level rise are the indirect drivers of soil salinity due to climate change in the studied lands. While the seawater seepage and drought were the direct factors for soil salinization in the studied lands. To ensure food security, the adaptation measures to climate change in the agricultural sector are highly needed which include incremental, systemic, and transformational changes at the farm scales. The incremental measures within the current farm system include planting times, improved seeding techniques, soil conservation, soil nutrient management, pest management, etc. while the systemic measures include climate-ready varieties, crop diversification, upscaling the farming, farm mechanization, efficient irrigation method, etc. The transformational measures are locational change in the agricultural field, a new crop system with changes in land use, farm location, and policy structure on a large scale. All three adaptation types should be followed in the present study lands and transformational adaptation should be started first followed by incremental, systemic adaptations. Expectations associated with the interactions of soil-climate, water-climate, and crop-climate relations should be taken into account in Egyptian farming at a larger scale, particularly in the drought-prone areas under saline conditions and climate change.

REFERENCES

Abdeen, M. M., A. Gaber, M. Shokr and O. A. El-Saadawy (2018). Minimizing labeling ambiguity during the classification process of the geological units covering the central part of the Suez Canal Corridor, Egypt using their radar scattering response. The Egyptian Journal of Remote Sensing and Space Sciences, 21, S55–S66.

Abdel-Kader, F. H. (2019). Assessment and monitoring of land degradation in the northwest coast region, Egypt using Earth observations data. J. Remote Sensing Space Sci., 22: 165–173.

Abuzied, S. M., M. F. Kaiser, E. H. Shendi and M. I. Abdel-Fattah (2020). Multi-criteria decision support for geothermal resources exploration based on remote sensing, GIS, and geophysical techniques along the Gulf of Suez coastal area, Egypt.

Ayres, R. S. and D. W. Westcott (1976). Water quality for agriculture. F.A.O. Irrigation and Drainage Paper No. 29 F.A.O. Rome.

Clesceri, L. S., A. E. Greenberg and A. D. Eaton (1998). Standard Methods for the Examination of Water and Wastewater, 20th ed. American Public Health Association, American Water Works Association, Water Environment Federation, United Book Press Inc., Baltimore, Maryland, USA.

Egyptian Meteorological Authority (2020). Climatic Atlas of Egypt, Cairo, Egypt.

Elwan, A. A. (2013). Novel approaches of land evaluation using geospatial technologies for planning sustainable development of desert areas. Ph.D. (Agric.) Thesis, Tamil Nadu Agric. Univ., Coimbatore, India, pp, 294.

Elwan, A. A. (2019). Dry Lands, Biodiversity, Management, and Conservation. *LC ebook* Chapter No. 9: Proper Evaluation of Desert Ecosystem for Sustainable Development. *Environmental Research Advances.* Nova Science Publishers, Inc., New York.

Eswar, D., R. Karuppusamy and S. Chellamuthu (2021). Drivers of soil salinity and their correlation with climate change. Current Opinion in Environmental Sustainability, 50: 310–318.

FAO (1976). A framework for land evaluation. Soils Bulletin No. 32. FAO, Rome, Italy.

FAO (2006). Guidelines for Soil Description. fourth ed., pp. 1-98 Rome.

FAO (2007). Land evaluation, towards a revised framework. Land and water discussion paper 6. FAO, Rome, Italy.

Field, C. B., V. R. Barros, D. J. Dokken, K. J. Mach, M. D. Mastrandrea and T. E. Bilir (2014). Climate change 2014 impacts, adaptation and vulnerability: Part A: Global and sectoral aspects: Working group II contribution to the fifth assessment report of the intergovernmental panel on climate change. Cambridge & New York: Cambridge University Press.

Hereher, M. E. (2018). Geomorphology and drift potential of major aeolian sand deposits in Egypt. Geomorphology, 304: 113–120

Hoover, D. J., K. O. Odigie, P. W. Swarzenski and P. Barnard (2017). Sea-level rise and coastal groundwater inundation and shoaling at select sites in California, USA. J Hydrol Reg Stud, 11: 234-249.

Kumar, H. V., M. Shivamurthy, M. M. Lunagaria (2017). Rainfall Trend Analysis and Adaptation Strategies to Manage Climate-Induced Crisis in Coastal Zone of Karnataka, India. Journal of Scientific Research and Reports, 1-11.

Ma, L., S. Yang, Z. Simayi, Q. Gu, J. Li, X. Yang and J. Ding (2018). Modeling variations in soil salinity in the oasis of Junggar Basin. China Land Degrad Dev, 29: 551-562.

Martínkovà, J., T. Hajek, L. Adamec and J. Klimesova (2021). Growth, root respiration and photosynthesis of a root-sprouting short-lived herb after severe biomass removal, Flora, 284: 151915.

Mukhopadhyay, R., B. Sarkar, H. S. Jat, P. C. Sharma and N. S. Bolan (2021). Soil salinity under climate change: Challenges for sustainable agriculture and food security. Journal of Environmental Management, 280: 111736.

Naylor, D., N. Sadler, A. Bhattacharjee, E. B. Graham, C. R. Anderton, R. McClure, M. Lipton, K. S. Hofmockel and J. K. Jansson (2020). Soil microbiomes under climate change and implications for carbon cycling. Annu. Rev. Environ. Resour, 45.

Omar, M. M., A. M. A. Moussa and R. Hinkelmann (2021). Impacts of climate change on water quantity, water salinity, food security, and socioeconomy in Egypt. Water Science and Engineering, 14(1): 17-27.

Panda, A. (2018). Transformational adaptation of agricultural systems to climate change. Wiley Interdisciplinary Reviews: Climate Change 9 (4), e520.

Perri, S., S. Suweis, D. Entekhabi and A. Molini (2018). Vegetation controls on dryland salinity. Geophys Res Lett, 45: 11669-11682.

Platt, R. V., M. Ogra, N. Kisak, U. Manral and R. Badola (2020). Climate change perceptions, data, and adaptation in the Garhwal Himalayas of India. Clim. Dev., 1–12. doi: 10.1080/17565529.2020.1724069.

Pörtner, H. O., D. C. Roberts, V. Masson-Delmotte, P. Zhai, M. Tignor, E. Poloczanska, K. Mintenbeck, A. Alegrıa, M. Nicolai, A. Okem and J. Petzold (2019). IPCC Special Report on the Ocean and Cryosphere in a Changing Climate (SROCC).

Rahman, M. S., L. Di, G. Y. Eugene, J. Tang, L. Lin, C. Zhang, Z. Yu and J. Gaigalas (2018). Impact of climate change on soil salinity: a remote sensing-based investigation in Coastal Bangladesh. 7th International Conference on Agro-geoinformatics (Agrogeoinformatics), 1-5.

Ruiz-Fernàndez, A. C., V. Carnero-Bravo, J. A. Sanchez-Cabeza, L. H. Perez-Bernal, O. A. Amaya-Monterrosa, S. Bojórquez-Sànchez, P. G. Lopez-Mendoza, J. G. Cardoso-Mohedano, R. B. Dunbar, D. A. Mucciarone and A. J. Marmolejo-Rodrıguez (2018). Carbon burial and storage in tropical salt marshes under the influence of sea level rise. Sci. Total Environ., 630: 1628-1640.

Shalby, A., M. Elshemy and B. A. Zeidan (2021). Modeling of climate change impacts on Lake Burullus, coastal lagoon (Egypt). Int. J. Sediment Res., 36(6): 756–769.

Soil Science Division Staff (2017). Soil survey manual. United States Department of Agriculture (USDA), Agriculture Handbook No. 18. Natural Resources Conservation Service, Washington, D.C, USA.

Soil Survey Staff (2014). Kellogg Soil Survey Laboratory methods manual. Soil Survey Investigations Report No. 42, version 5.0. R. Burt and Soil Survey Staff (eds.). U.S. Department of Agriculture-Natural Resources Conservation Service. Washington DC, USA.

Wang, F., S. Yang, Y. Wei, Q. Shi and J. Ding (2021). Characterizing soil salinity at multiple depths using electromagnetic induction and remote sensing data with random forests: a case study in Tarim River Basin of southern Xinjiang, China. Sci. Total Environ., 754: 142030.

WMO (2017). World Meteorological Organization (WMO) Statement on the State of the Global Climate in 2016. WMO, Geneva.

Yassen, A. N. W. Nam and E. Hong (2020). Impact of climate change on reference evapotranspiration in Egypt. Catena, 194: 104711.

Younis, A. M., N. F. Soliman and E. M. Elkady (2021). Distribution and ecological risk evaluation of bioavailable phosphorus in sediments of El Temsah Lake, Suez Canal, Oceanologia, https://doi.org/10.1016/j.oceano.2021.12.001.

Zhang, X., Z. Zhang, W. Wang, W. Fang, Y. Chiang, X. Liu and H. Ju. (2021). Vegetation successions of coastal wetlands in southern Laizhou Bay, Bohai Sea, northern China, influenced by the changes in relative surface elevation and soil salinity. Journal of Environmental Management, 293: 112964.

تأثير تسرب مياه قناة السويس الجديدة على خواص التربة بمنطقة الأمل، شرق الإسماعيلية، مصر

عادل عبدالحميد علوان خليل
قسم البيدولوچي، شعبة مصادر المياه والأراضي الصحراوية، مركز بحوث الصحراء، المطرية – رقم بريدي ١١٧٥٣، القاهرة

أُجريت الدراسة على مساحة ٢٨٥ فدان بمنطقة الأمل بشرق الإسماعيلية في عام ٢٠٢٠، كنموذج للأراضي الساحلية المصرية والمُتاخمة لقطاع قناة السويس الجديدة، حيث تبعد عن مجرى القناة بحوالي ٢ كيلومترات أو يزيد قليلاً. إهتمت الدولة المصرية في الآونة الأخيرة بتطبيقات البحث العلمي وإنخراطه بالمشروعات القومية الزراعية، وذلك من خلال تكثيف الدراسات العلمية الحديثة والدقيقة في ظل التغيرات العالمية خاصة التغير المناخي Climate change وتأثيره على الزراعة بالمناطق الساحلية المصرية. يهدف البحث إلى دراسة تأثير تسرب مياه البحار وخاصة مياه قناة السويس الجديدة إلى الأراضي المنخفضة بنطاق السواحل المزروعة بالفعل والمُتاخمة لمجرى قناة السويس مع التركيز على التغيرات التي طرأت على صفات التربة البيدومورفولوچية والفيزيائية والكيميائية، وتحديد العوامل Drivers التي أدت إلى هذه التغيرات، مع التأكيد على إتباع تدابير مُعينة للتكيف مع التغيرات المناخية تتلائم مع أسباب تدهور التربة ودرجة وكثافة المّحدات الزراعية. ولتحقيق هذه الأهداف؛ تم إجراء حصر تفصيلي للموارد الأرضية تحت الدراسة Detailed soil survey من خلال حفر القطاعات الأرضية والدراسة البيدومورفولوچية ومن ثم تجميع عينات التربة المُمثلة لطبقات القطاع الأرضي، للوقوف على أهم الصفات الطبيعية والكيميائية لهذه الموارد الأرضية وكذلك تم أخذ عينات المياه أثناء حفر قطاعات التربة عند مستويات مُختلفة من منسوب الماء الأرضي Water Table للتعرف على الصفات الكيميائية للماء الأرضي. وقد لوحظ أن الأراضي تحت الدراسة لا يزيد ارتفاعها عن ١١ متر فوق مستوى سطح البحر. تم التعرف على منطقة السبخات والمستنقعات الملحية والتي تم غمرها بمياه قناة السويس المالحة بشكل جزئي إلى كامل، وتغطي مساحة تصل إلى ٤٥,٤ فدان؛ حيث لوحظ التشبع الكامل لكافة طبقات القطاع الأرضي. بعد استبعاد منطقة السبخات، تم تقسيم المساحة المتبقية من منطقة الدراسة (٢٣٩,٦ فدان) إلى خمس وحدات أرضية خرائطية (Soil Mapping Units (SMUs. كما تم الإشارة بشكل موجز إلى درجة صلاحية التربة بمنطقة الدراسة، فقد خُلصت النتائج إلى صلاحية أراضي الوحدات الخرائطية الأولى والثانية والثالثة للزراعة، والتي تصل مساحتها إلى ٦٧,٨ فدان فقط وهي تمثل التربة العميقة. كما أوضحت النتائج سيادة الأراضي غير الصالحة للزراعة والتي تمتد على مساحة تصل إلى ٢١٧,٢ فدان بنسبة ٧٦,٢% من إجمالي مساحة منطقة الدراسة (٢٨٥ فدان) ، حيث تشمل الأراضي غير الصالحة للزراعة كلاً من: أرضي السبخات (٤٥,٤ فدان)، والوحدة الخرائطية الرابعة متوسطة العمق (٤٨,٨ فدان)، والوحدة الخرائطية الخامسة الضحلة (١٢٣ فدان) بعد ما كانت صالحة للإنتاج الزراعي لبعض المحاصيل الحقلية وأشجار الفاكهة خلال السنوات القليلة السابقة، حيث تدهورت مؤخراً نتيجة لزيادة تداخل المياه المالحة لقناة السويس خلال طبقات قطاعات التربة تحت الدراسة، والتي أدت إلى التشبع الكامل بمياه شديدة الملوحة وتحولها إلى بيئة متدهور ومُتصحرة وامتلاكها المعوقات شديدة الحدة والمتعلقة بارتفاع الملوحة الأرضية وسوء الصرف بصورة دائمة، بالإضافة إلى التدهور الفيزيائي لخواص التربة بسبب التدهور الكامل لبناء التربة نتيجة سيادة كاتيونات الصوديوم معقد التبادل في حبيبات التربة مما أدى إلى تفرقها وتحطيم البناء الأرضي وانسداد المسام الهوائية وتشبعها الكامل بالمياه المالحة. أدى ذلك إلى إختلال الميزان المائي الهوائي للتربة حيث يتوقع نقص نسبة الأوكسچين اللازم لتنفس جذور النباتات، مع ارتفاع ملوحة التربة والتي وصلت إلى ٢٩,٦٠ ديسيمنز/م، حيث إعاقة نمو المحاصيل بها وجفافها بصورة كاملة. ارتفاع الماء الأرضي المالح أدى إلى تشبع معظم طبقات قطاع التربة، والذي ترتب عليه التدهور الكامل ليشمل كافة صفات التربة المختلفة. أكدت نتائج الدراسة أن الوحدات الخرائطية الأولى والثانية (SMU 1 and SMU 2) التي تقع على ارتفاعات في المدى ٩-١١ متر فوق مستوى سطح البحر لم تتأثر (ولو بشكل مؤقت) بتسرب المياه المالحة Seawater بينما تأثرت تربة الوحدات الخرائطية الثالثة، الرابعة ، والخامسة (SMU 3, SMU 4 and SMU 5) التي ترتفع عن مستوى سطح البحر بمقدار ٧-٨ متر، بينما تحولت التربة التي يقل إرتفاعها عن منسوب سطح البحر بمقدار ٧ متر إلى مستنقعات ملحية وسبخات. حيث وجد أن منطقة الدراسة بمزرعة الأمل أكثر عُرضة لتأثير التغيرات المناخية Climate changes. وبناءاً عليه؛ فإنه يتوقع إستمرار عملية التسريب الأفقي لمياه قناة السويس الجديدة لتشمل بعض الأراضي المجاورة الصالحة للزراعة حالياً بالمنطقة، وكذلك للمناطق التي تبعد عن مجرى القناة بمسافة تصل إلى٣ كم، وهنا يجدر الإشارة إلى مراقبة ومُتابعة منسوب الماء الأرضي لهذه الأراضي المجاورة، وكذلك المُتابعة الدورية لخواص التربة الكيميائية والطبيعية باستمرار، والعمل على توفير الصرف الجيد للتربة خوفاً من تدهور خواصها المائية والتي يترتب عليها تدهور باقي الصفات الأخرى للتربة الزراعية. وبناءاً على المُحدات الزراعية ولضغوط تغير المناخ الحادة، فإنه يجب اتخاذ كافة الإجراءات الوقائية والتي تخفف أو تتكيف مع التغيرات العالمية والتقلبات الجوية الحادة، وأهم تلك الإجراءات هي التي تتعلق باتخاذ كافة تدابير التكيف Adaptation measures مع عوامل التغير المناخي في قطاع الزراعة خاصة فيما يتعلق بإدارة التربة – المياه – النبات، والتي من أهمها (أ): ممارسات تدريجية Incremental practicesوهي تكمن داخل المزرعة مثل التغير في مواعيد الزراعة ومسافة الزراعة، إجراءات صيانة التربة، إدارة مياه الري ومغذيات ووقاية النبات، وغيرها، (ب): إجراءات نظامية Systemic measures حيث التغير الجزئي في نظام المزرعة مثل إتباع كافة أنواع التكنولوچيا من أول بذر البذور حتى الحصاد، التحول إلى استنباط أصناف من المحاصيل المتحملة للجفاف والملوحة Shift to climate-ready varieties، الإرتقاء بالمزرعة Upscaling the farming، إدارة مُحسنة لمكافحة الآفات الزراعية Improved pest management، إدخال طريقة فعالة للري Incorporation of efficient irrigation method، ميكنة المزرعة Farm mechanization، وأخيرا (ج): التدابير التحويلية Transformational measures والتي تشمل كافة التدابير لنقل مكان المزرعة إلى المناطق الأكثر أماناً ضد تسرب مياه البحار، حيث إتباع الممارسات التي تهدف إلى تغير كلي ومكاني في نظام المزرعة Locational change of the farm and agricultural field حتى يتم التكيف مع التذبذب الحاد في المناخ الذي ينتج عنه تأثير مباشر على وحدتي التربة والمياه، وبالتالي إنتاجية المحاصيل، خاصة في المناطق الأكثرعُرضة للجفاف والتملح كما هو الحال في منطقة الدراسة. وبناءاً عليه؛ أوصت هذه الدراسة بإستخدام كافة أنواع التدابير الثلاثة السابقة وخاصة البدء بالتدابير التحويلية Transformational measures والتي تهدف إلى تغير الإستخدام الأرضي Land-use change ، يليها التدابير الأخرى Incremental and systemic actions في حالة المنطقة تحت الدراسة، حيث تعتبر التدابير التحويلية Transformational measures هي أفضل الممارسات والأكثر فعالية للأراضي تحت الدراسة للحصول على أعلى تكيفاً مع التغيرات المناخية الحالية نظراً لتأثر أراضي منطقة الدراسة بمُحدات أرضية عالية Soil limitations وضغوط شديدة Stressors تتعلق بتملح التربة، ومشاكل الصرف، والتشبع الدائم لطبقات قطاع التربة بالماء المالح، بالاضافة إلى تأثر المنطقة بالجفاف، وإرتفاع درجات الحرارة وقلة مياه الأمطار. وعليه، فلابد من إعادة التخطيط الجيد لإستخدامات أراضي المناطق الساحلية المصرية، وإستخدام تلك المناطق للأنشطة غير الزراعية ذات المردود الإقتصادي العالي، بحيث يتم تفادي مثل هذه التحديات والتغيرات المناخية العالمية.